Multiscale discrete approximations of Fourier integral operators associated with canonical transformations and caustics

Maarten van de Hoop, Gunther Uhlmann, Andras Vasy, Herwig Wendt

MULTISCALE DISCRETE APPROXIMATIONS OF FOURIER INTEGRAL OPERATORS ASSOCIATED WITH CANONICAL TRANSFORMATIONS AND CAUSTICS*

MAARTEN V. DE HOOP[†], GUNTHER UHLMANN[‡], ANDRÁS VASY[§], AND
HERWIG WENDT[¶]

Abstract. We develop an algorithm for the computation of general Fourier integral operators associated with canonical graphs. The algorithm is based on dyadic parabolic decomposition using wave packets and enables the discrete approximate evaluation of the action of such operators on data in the presence of caustics. The procedure consists of constructing a universal operator representation through the introduction of locally singularity-resolving diffeomorphisms, thus enabling the application of wave packet–driven computation, and of constructing the associated pseudodifferential joint-partition of unity on the canonical graphs. We apply the method to a parametrix of the wave equation in the vicinity of a cusp singularity.

Key words. Fourier integral operators, caustics, multiscale computations, wave packets, dyadic parabolic decomposition, operator compression, reflection seismology

1. Introduction. In this paper, we develop an algorithm for applying Fourier integral operators associated with canonical graphs using wave packets. To arrive at such an algorithm, we construct a universal oscillatory integral representation of the kernels of these Fourier integral operators by introducing singularity-resolving diffeomorphisms where caustics occur. The universal representation is of a form such that the algorithm based on the dyadic parabolic decomposition of phase space previously developed by the authors applies [2]. We refer to [7, 8, 10, 11] for related computational methods aiming at the evaluation of the action of Fourier integral operators.

The algorithm comprises a geometrical component, bringing the local representations in universal form, and a wave packet component, which yields the application of the local operators. Here, we develop the geometrical component, which consists of the following steps. First we determine the location of caustics on the canonical relation of the Fourier integral operator. For each point on a caustic we determine the associated specific rank deficiency and construct an appropriate diffeomorphism, resolving the caustic in open neighborhoods of this point. We determine the (local) phase function of the composition of the Fourier integral operator and the inverse of the diffeomorphism in terms of universal coordinates and detect the largest set on

which it is defined. We evaluate the preimage of this set on the canonical relation. We continue this procedure until the caustic is covered with overlapping sets, associated with diffeomorphisms for the corresponding rank deficiencies. Then we repeat the steps for each caustic and arrive at a collection of open sets covering the canonical relation.

In the special case of Fourier integral operators corresponding to parametrices of evolution equations, for isotropic media, an alternative approach for obtaining solutions in the vicinity of caustics, based on a redecomposition strategy following a multiproduct representation of the propagator, has been proposed previously [2, 19, 20]. Unlike multiproduct representations, our construction does not involve a subdivision of the evolution parameter and yields a single-step computation. Moreover, it is valid for the general class of Fourier integral operators associated with canonical graphs, allowing for anisotropy.

The complexity of the algorithm for general Fourier integral operators as compared to the noncaustic case arises from switching, in the sets covering a small neighborhood of the caustics, from a global to a local algorithm using a pseudodifferential partition of unity.

As an application we present the computation of a parametrix of the wave equation in a heterogeneous, isotropic setting for long-time stepping in the presence of caustics.

Curvelets, wave packets. We briefly discuss the (co)frame of curvelets and wave packets [9, 13, 24]. Let $u \in L^2(\mathbb{R}^n)$ and consider its Fourier transform, $\hat{u}(\xi) = \int u(x) \exp[-\mathrm{i}\langle x, \xi \rangle] \, dx$.

One begins with an overlapping covering of the positive ξ_1 axis ($\xi' = \xi_1$) by boxes of the form

$$(1.1) \qquad B_k = \left[\xi'_k - \frac{L'_k}{2}, \xi'_k + \frac{L'_k}{2} \right] \times \left[-\frac{L''_k}{2}, \frac{L''_k}{2} \right]^{n-1},$$

where the centers ξ'_k, as well as the side lengths L'_k and L''_k, satisfy the parabolic scaling condition

$$\xi'_k \sim 2^k, \quad L'_k \sim 2^k, \quad L''_k \sim 2^{k/2} \quad \text{as } k \to \infty.$$

Next, for each $k \geq 1$, let ν vary over a set of $\sim 2^{k(n-1)/2}$ uniformly distributed unit vectors. Let $\Theta_{\nu,k}$ denote a choice of rotation matrix which maps ν to e_1 and $B_{\nu,k} = \Theta_{\nu,k}^{-1} B_k$. In the (co-)frame construction, one encounters two sequences of smooth functions on $\mathbb{R}^n$, $\hat{\chi}_{\nu,k}$ and $\hat{\beta}_{\nu,k}$, each supported in $B_{\nu,k}$, so that they form a co-partition of unity, $\hat{\chi}_0(\xi)\hat{\beta}_0(\xi) + \sum_{k \geq 1} \sum_\nu \hat{\chi}_{\nu,k}(\xi)\hat{\beta}_{\nu,k}(\xi) = 1$, and satisfy the estimates

$$|\langle \nu, \partial_\xi \rangle^j \partial_\xi^\alpha \hat{\chi}_{\nu,k}(\xi)| + |\langle \nu, \partial_\xi \rangle^j \partial_\xi^\alpha \hat{\beta}_{\nu,k}(\xi)| \leq C_{j,\alpha} \, 2^{-k(j+|\alpha|/2)}.$$

One then forms $\hat{\psi}_{\nu,k}(\xi) = \rho_k^{-1/2} \hat{\beta}_{\nu,k}(\xi)$, $\hat{\varphi}_{\nu,k}(\xi) = \rho_k^{-1/2} \hat{\chi}_{\nu,k}(\xi)$, with $\rho_k = \mathrm{vol}(B_k)$, satisfying the estimates

$$(1.2) \qquad \forall N: \quad \left. \begin{array}{c} |\varphi_{\nu,k}(x)| \\ |\psi_{\nu,k}(x)| \end{array} \right\} \leq C_N 2^{k(n+1)/4} \left(2^k |\langle \nu, x \rangle| + 2^{k/2} \|x\| \right)^{-N}.$$

To obtain a (co)frame, one introduces the integer lattice, $X_m := (m_1, \ldots, m_n) \in \mathbb{Z}^n$; the dilation matrix, $D_k = \frac{1}{2\pi} \left(\begin{smallmatrix} L'_k & 0_{1 \times n-1} \\ 0_{n-1 \times 1} & L''_k I_{n-1} \end{smallmatrix} \right)$; $\det D_k = (2\pi)^{-n} \rho_k$; and points $x_m^{\nu,k} =$

$\Theta_{\nu,k}^{-1}D_k^{-1}X_m$. The frame elements ($k \geq 1$) are then defined in the Fourier domain as $\hat{\varphi}_\gamma(\xi) = \hat{\varphi}_{\nu,k}(\xi) \exp[-\mathrm{i}\langle x_m^{\nu,k}, \xi\rangle]$, $\gamma = (m, \nu, k)$, and similarly for $\hat{\psi}_\gamma(\xi)$. The function $\varphi_{\nu,k}$ is referred to as a wave packet. One obtains the transform pair

$$(1.3) \qquad u_\gamma = \int u(x)\overline{\psi_\gamma(x)}\,\mathrm{d}x, \qquad u(x) = \sum_\gamma u_\gamma \varphi_\gamma(x).$$

2. Fourier integral operators and caustics. We consider Fourier integral operators, F, associated with canonical graphs. We allow the formation of caustics.

2.1. Oscillatory integrals, local coordinates. Let (y, x_{I_i}, ξ_{J_i}) be local coordinates on the canonical relation, Λ say, of F, and S_i a corresponding generating function: If, at a point on Λ, (dy, dx_I) are linearly independent and dx_J vanishes, then $(dy, dx_I, d\xi_J)$ are coordinates on Λ nearby, $I \cup J = \{1, \ldots, n\}$, $I \cap J = \{\emptyset\}$, and one can parameterize Λ as $\langle X_J(y, x_I, \xi_J) - x_J, \xi_J\rangle$, where $x_J = X_J(y, x_I, \xi_J)$ locally on Λ (cf. [18, Thm. 21.2.18]). The fact that a (possibly empty) set I exists follows from the canonical graph property, i.e., that (y, η) are local coordinates and dy linearly independent. Then

$$x_{J_i} = \frac{\partial S_i}{\partial \xi_{J_i}}, \qquad \xi_{I_i} = -\frac{\partial S_i}{\partial x_{I_i}},$$
$$(2.1)$$
$$\eta = \frac{\partial S_i}{\partial y}.$$

The coordinates are defined in a standard way on (overlapping) open sets O_i in Λ, that is, $(y, x_{I_i}, \xi_{J_i}) \to r(y, x_{I_i}, \xi_{J_i})$ is defined as a diffeomorphism on O_i; let $i = 1, \ldots, N$. The corresponding partition of unity is written as

$$(2.2) \qquad \sum_{i=1}^N \Gamma_i(r) = 1, \quad r \in \Lambda.$$

In local coordinates, we introduce

$$(2.3) \qquad \bar{\Gamma}_i(y, x_{I_i}, \xi_{J_i}) = \Gamma_i(r(y, x_{I_i}, \xi_{J_i})).$$

Then $(F\varphi_\gamma)(y) = \sum_{i=1}^N (F_i \varphi_\gamma)(y)$ with

$$(2.4)$$
$$(F_i \varphi_\gamma)(y)$$
$$= \int\int \bar{\Gamma}_i(y, x_{I_i}, \xi_{J_i}) a_i(y, x_{I_i}, \xi_{J_i}) \exp[\mathrm{i}\underbrace{(S_i(y, x_{I_i}, \xi_{J_i}) - \langle \xi_{J_i}, x_{J_i}\rangle)}_{\phi(y, x, \xi_{J_i})}]\, \varphi_\gamma(x)\,\mathrm{d}x\mathrm{d}\xi_{J_i}.$$

The amplitude $a_i(y, x_{I_i}, \xi_{J_i})$ is complex and accounts for the KMAH (Keller–Maslov–Arnold–Hörmander; cf. [25]) index.

We let Σ_ϕ denote the stationary point set (in θ) of $\phi = \phi(y, x, \theta)$. The amplitude can be identified with a half-density on Λ. One defines the $2n$-form d_ϕ on Σ_ϕ,

$$d_\phi \wedge d\left(\frac{\partial\phi}{\partial\theta_1}\right) \wedge \cdots \wedge d\left(\frac{\partial\phi}{\partial\theta_N}\right) = dy_1 \wedge \cdots \wedge dy_n \wedge dx_1 \wedge \cdots \wedge dx_n \wedge d\theta_1 \wedge \cdots \wedge d\theta_N.$$

In the above, we choose $\lambda = (y, x_I, \frac{\partial\phi}{\partial x_J})$ as local coordinates on Λ, while $\theta = \xi_J$. Then we get

$$d_\phi = |\Delta_\phi|^{-1}|d\lambda_1 \wedge \cdots \wedge d\lambda_{2n}|, \qquad \Delta_\phi = \begin{vmatrix} \frac{\partial^2\phi}{\partial x_J\partial x_J} & \frac{\partial^2\phi}{\partial \xi_J\partial x_J} \\ \frac{\partial^2\phi}{\partial x_J\partial \xi_J} & \frac{\partial^2\phi}{\partial \xi_J\partial \xi_J} \end{vmatrix} = -1;$$

λ is identified with (y, x_I, ξ_J). The corresponding half-density equals $|\Delta_\phi|^{-1/2}|d\lambda_1 \wedge \cdots \wedge d\lambda_{2n}|^{1/2}$.

Densities on a submanifold of the cotangent bundle are associated with the determinant bundle of the cotangent bundle. Let a_i^0 denote the leading-order homogeneous part of a_i. The principal symbol of the Fourier integral operator then defines a half-density, $a_i^0 d_\phi^{1/2}$. That is, for a change of local coordinates, if the transformation rule for forms of maximal degree is the multiplication by a Jacobian $\jmath$, then the transformation rule for a half-density is the multiplication by $|\jmath|^{1/2}$. In our case, of canonical graphs, we can dispose of the description in terms of half-densities and restrict to zero-density amplitudes on Λ.

2.2. Propagator. The typical case of a Fourier integral operator associated with a canonical graph is the parametrix for an evolution equation [14, 15],

$$(2.5) \qquad [\partial_t + iP(t, x, D_x)]u(t, x) = 0, \quad u(t_0, x) = \varphi_\gamma(x),$$

on a domain $X \subset \mathbb{R}^n$ and a time interval $[t_0, T]$, where $P(t, x, D_x)$ is a pseudodifferential operator with symbol in $S_{1,0}^1$; we let p denote the principal symbol of P.

For every $(x, \xi) \in T^*X \setminus \{0\}$, the integral curves $(y(x, \xi; t, t_0), \eta(x, \xi; t, t_0))$ of

$$(2.6) \qquad \frac{dy}{dt} = \frac{\partial p(t, y, \eta)}{\partial \eta}, \quad \frac{d\eta}{dt} = -\frac{\partial p(t, y, \eta)}{\partial y},$$

with initial conditions $y(x, \xi; t_0, t_0) = x$ and $\eta(x, \xi; t_0, t_0) = \xi$, define the transformation, χ, from (x, ξ) to (y, η), which generates the canonical relation of the parameterix of (2.5), for a given time $t = T$; that is, $(y(x, \xi), \eta(x, \xi)) = (y(x, \xi; T, t_0), \eta(x, \xi; T, t_0))$.

The perturbations of (y, η) with respect to initial conditions (x, ξ) are collected in a propagator matrix,

$$(2.7) \qquad \Pi(x, \xi; t, t_0) = \begin{pmatrix} W_1 & W_2 \\ W_3 & W_4 \end{pmatrix} = \begin{pmatrix} \partial_x y & \partial_\xi y \\ \partial_x \eta & \partial_\xi \eta \end{pmatrix},$$

which is the solution to the $2n \times 2n$ system of differential equations

$$(2.8) \qquad \frac{d\Pi}{dt}(x, \xi; t, t_0) = \begin{pmatrix} \dfrac{\partial^2 p}{\partial \eta \partial y}(t, y, \eta) & \dfrac{\partial^2 p}{\partial \eta \partial \eta}(t, y, \eta) \\ -\dfrac{\partial^2 p}{\partial y \partial y}(t, y, \eta) & -\dfrac{\partial^2 p}{\partial y \partial \eta}(t, y, \eta) \end{pmatrix} \Pi(x, \xi; t, t_0),$$

known as the Hamilton–Jacobi equations, supplemented with the initial conditions [25, 26]

$$(2.9) \qquad \Pi(x, \xi; t_0, t_0) = \begin{pmatrix} \mathbb{I} & 0 \\ 0 & \mathbb{I} \end{pmatrix}.$$

Away from caustics the generating function of Λ is $S = S(y, \xi)$ ($I_i = \emptyset$), which satisfies

$$(2.10) \qquad \frac{\partial^2 S}{\partial y \partial \xi}(y, \xi) = \frac{\partial x}{\partial y}\bigg|_\xi = W_1^{-1},$$

$$(2.11) \qquad \frac{\partial^2 S}{\partial \xi^2}(y, \xi) = \frac{\partial x}{\partial \xi}\bigg|_y = -\frac{\partial x}{\partial y}\bigg|_\xi \frac{\partial y}{\partial \xi}\bigg|_y = -W_1^{-1}W_2,$$

$$(2.12) \qquad \frac{\partial^2 S}{\partial y^2}(y, \xi) = \frac{\partial \eta}{\partial y}\bigg|_\xi = \frac{\partial \eta}{\partial x}\bigg|_\xi \frac{\partial x}{\partial y}\bigg|_\xi = W_3 W_1^{-1},$$

where $x = x(y, \xi; t_0, T)$ denotes the backward solution to (2.6) with initial time T, evaluated at t_0. The leading-order amplitude is then

$$(2.13) \qquad a(y, \xi/|\xi|) = \sqrt{1/\det W_1(x(y, \xi/|\xi|; t_0, T), \xi/|\xi|; T, t_0)},$$

reflecting that a is homogeneous of degree 0 in ξ.

In the vicinity of caustics, we need to choose different coordinates. Admissible coordinates are directly related to the possible rank deficiency of W_1: One determines the null space of the matrix W_1 and rotates the coordinates such that the null space is spanned by the columns indexed by the set I_i. Then (y, x_{I_i}, ξ_{J_i}) form local coordinates on the canonical relation Λ, as in the previous subsection, and O_i is given by the set for which the columns indexed by I_i span the null space of W_1.

3. Singularity-resolving diffeomorphisms. We consider the matrix $W_1(x(y, \xi; t_0, T), \xi; T, t_0)$ for given (T, t_0) at $y_0 = y(x_0, \xi_0; T, t_0)$ and $\xi = \xi_0$ and determine its rank. Suppose it does not have full rank at this point. We construct a diffeomorphism which removes this rank deficiency in a neighborhood of $r_0 = (y_0, \eta_0; x_0, \xi_0) \in \Lambda$, where $\eta_0 = \eta(x_0, \xi_0; T, t_0)$.

To be specific, we rotate coordinates such that $\xi_0 = (1, 0, \ldots, 0)$ (upon normalization). Let us assume that the row associated with the coordinate x_2 generates the rank deficiency. (There could be more than one row / coordinate.) We then introduce the diffeomorphism

$$Q : x \mapsto \tilde{x} = \left(x_1 - \frac{\alpha}{2}(x_2 - (x_0)_2)^2, x_2, \ldots, x_n \right);$$

to preserve the symplectic form, we map

$$\xi \mapsto \tilde{\xi} = (\xi_1, \xi_2 + \alpha(x_2 - (x_0)_2)\, \xi_1, \xi_3, \ldots, \xi_n),$$

yielding a canonical transformation $C_Q : (x, \xi) \mapsto (\tilde{x}, \tilde{\xi})$. We note that $C_Q(x_0, \xi_0) = (x_0, \xi_0)$.

The canonical transformation, C_Q^{-1}, associated with Q^{-1} is given by

$$\tilde{x} \to x = \left(\tilde{x}_1 + \frac{\alpha}{2}(\tilde{x}_2 - x_{0,2})^2, \tilde{x}_2, \ldots, \tilde{x}_n \right),$$

$$\tilde{\xi} \to \xi = (\tilde{\xi}_1, \tilde{\xi}_2 - \alpha(\tilde{x}_2 - x_{0,2})\, \tilde{\xi}_1, \ldots, \tilde{\xi}_n).$$

We introduce the pull back, $Q^* u(\tilde{x}) = u(Q^{-1}(\tilde{x})) = u(\tilde{x}_1 + \frac{\alpha}{2}(\tilde{x}_2 - (x_0)_2)^2, \tilde{x}_2, \ldots, \tilde{x}_n)$.

3.1. Fourier integral representations of Q and Q^{-1}. The diffeomorphism Q can be written in the form of an invertible Fourier integral operator with unit amplitude and canonical relation given as the graph of C_Q. To see this, we write $(Q^* u)(\tilde{x}) = u(X(\tilde{x}))$, $((Q^{-1})^* \tilde{u})(x) = \tilde{u}(\tilde{X}(x))$. That is, $X = Q^{-1}$ and $\tilde{X} = Q$. The diffeomorphisms Q and Q^{-1} define the Fourier integral operators with oscillatory integral kernels,

$$(3.1) \qquad A_Q(\tilde{x}, x) = \int e^{-i\langle \xi, x - X(\tilde{x}) \rangle} \mathrm{d}\xi, \quad A_{Q^{-1}}(x, \tilde{x}) = \int e^{-i\langle \tilde{\xi}, \tilde{x} - \tilde{X}(x) \rangle} \mathrm{d}\tilde{\xi}.$$

The generating functions are

$$S_Q(\tilde{x}, \xi) = \langle \xi, X(\tilde{x}) \rangle, \quad S_{Q^{-1}}(x, \tilde{\xi}) = \langle \tilde{\xi}, \tilde{X}(x) \rangle,$$

respectively. The canonical relations are the graphs of C_Q and $C_{Q^{-1}}$ and are given by

$$\Lambda_Q = \{(\tilde{x} = X^{-1}(x), \langle \xi, \partial_{\tilde{x}} X \rangle|_{\tilde{x} = X^{-1}(x)}; x, \xi)\},$$
$$\Lambda_{Q^{-1}} = \{(x = \tilde{X}^{-1}(\tilde{x}), \langle \tilde{\xi}, \partial_x \tilde{X} \rangle|_{x = \tilde{X}^{-1}(\tilde{x})}; \tilde{x}, \tilde{\xi})\}.$$

The Hessians yield a unit amplitude:

$$\left| \det \frac{\partial^2 \langle \xi, X(\tilde{x}) \rangle}{\partial \tilde{x} \partial \xi} \right| = 1, \qquad \left| \det \frac{\partial^2 \langle \tilde{\xi}, \tilde{X}(x) \rangle}{\partial x \partial \tilde{\xi}} \right| = 1.$$

Substituting the particular diffeomorphism, we obtain

$$\partial_x \tilde{X}|_{x = \tilde{X}^{-1}(\tilde{x})} = \begin{pmatrix} 1 & -\alpha(\tilde{x}_2 - x_{0,2}) & 0 & \cdots \\ 0 & 1 & 0 & \cdots \\ 0 & 0 & 1 & \cdots \\ \vdots & \vdots & \vdots & \ddots \end{pmatrix},$$

$$\langle \tilde{\xi}, \partial_x \tilde{X} \rangle|_{x = \tilde{X}^{-1}(\tilde{x})} = \begin{pmatrix} \tilde{\xi}_1 \\ \tilde{\xi}_2 - \alpha(\tilde{x}_2 - x_{0,2})\tilde{\xi}_1 \\ \vdots \end{pmatrix}.$$

The corresponding propagator matrices are hence given by

(3.2)

$$\Pi_Q = \begin{pmatrix} \frac{\partial \tilde{x}}{\partial x} & \frac{\partial \tilde{x}}{\partial \xi} \\ \frac{\partial \tilde{\xi}}{\partial x} & \frac{\partial \tilde{\xi}}{\partial \xi} \end{pmatrix} = \begin{pmatrix} 1 & -\alpha(x_2 - x_{0,2}) & 0 & \cdots & 0 & 0 & 0 & \cdots \\ 0 & 1 & 0 & \cdots & 0 & 0 & 0 & \cdots \\ 0 & 0 & 1 & \cdots & 0 & 0 & 0 & \cdots \\ \vdots & \vdots & \vdots & \ddots & \vdots & \vdots & \vdots & \ddots \\ 0 & 0 & 0 & \cdots & 1 & 0 & 0 & \cdots \\ 0 & \alpha\xi_1 & 0 & \cdots & \alpha(x_2 - x_{0,2}) & 1 & 0 & \cdots \\ 0 & 0 & 0 & \cdots & 0 & 0 & 1 & \cdots \\ \vdots & \vdots & \vdots & \ddots & \vdots & \vdots & \vdots & \ddots \end{pmatrix},$$

(3.3)

$$\Pi_Q^{-1} = \begin{pmatrix} \frac{\partial x}{\partial \tilde{x}} & \frac{\partial x}{\partial \tilde{\xi}} \\ \frac{\partial \xi}{\partial \tilde{x}} & \frac{\partial \xi}{\partial \tilde{\xi}} \end{pmatrix} = \begin{pmatrix} 1 & \alpha(\tilde{x}_2 - x_{0,2}) & 0 & \cdots & 0 & 0 & 0 & \cdots \\ 0 & 1 & 0 & \cdots & 0 & 0 & 0 & \cdots \\ 0 & 0 & 1 & \cdots & 0 & 0 & 0 & \cdots \\ \vdots & \vdots & \vdots & \ddots & \vdots & \vdots & \vdots & \ddots \\ 0 & 0 & 0 & \cdots & 1 & 0 & 0 & \cdots \\ 0 & -\alpha\tilde{\xi}_1 & 0 & \cdots & -\alpha(\tilde{x}_2 - x_{0,2}) & 1 & 0 & \cdots \\ 0 & 0 & 0 & \cdots & 0 & 0 & 1 & \cdots \\ \vdots & \vdots & \vdots & \ddots & \vdots & \vdots & \vdots & \ddots \end{pmatrix},$$

which are easily verified to be symplectic matrices. In the more general case, each coordinate x_j generating a rank deficiency yields additional nonzero entry pairs $\frac{\partial \tilde{x}_1}{\partial x_j}$, $\frac{\partial x_1}{\partial \tilde{x}_j}$, $\frac{\partial \tilde{\xi}_j}{\partial x_j}$, $\frac{\partial \xi_j}{\partial \tilde{x}_j}$, and $\frac{\partial \tilde{\xi}_j}{\partial \xi_1}$, $\frac{\partial \xi_j}{\partial \tilde{\xi}_1}$ in the above propagator matrices.
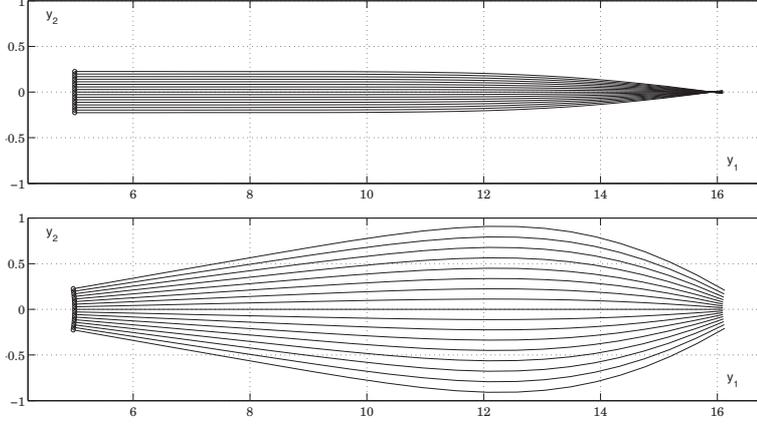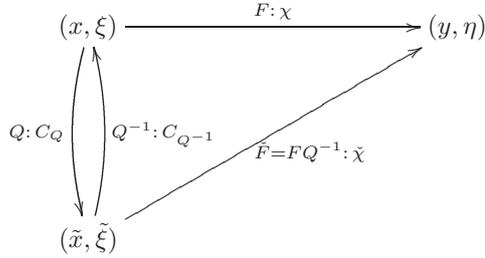
Fig. 1. *Illustration of canonical relations χ (top) and $\check{\chi}$ (bottom) of operators F and $\check{F}$ associated with a half-wave equation: (bi-)characteristics ("rays") in y for initial conditions $(x_2 = x_{2,0}, \ \xi = \xi_0)$ and $(\tilde{x}_2 = \tilde{x}_{2,0}, \ \tilde{\xi} = \tilde{\xi}_0)$, respectively, for evolution through a low velocity lens (see section 5). The black circles on the left indicate the conjugate points corresponding to the initial conditions.*

3.2. Operator composition. It follows that the composition $(\tilde{x}, \tilde{\xi}) \overset{C_Q^{-1}}{\mapsto} (x, \xi) \overset{\chi}{\mapsto} (y, \eta)$ generates the graph of a canonical transformation, $\check{\chi}$ say, which can be parametrized by $(y, \tilde{\xi})$ locally on an open neighborhood of $(y_0, \tilde{\xi}(x_0, \xi_0))$ (see Figure 1 for an illustration). We denote the corresponding generating function by $\check{S} = \check{S}(y, \tilde{\xi})$. We can compose F with Q^{-1} as Fourier integral operators: $\check{F} = FQ^{-1}$. The canonical relation of $\check{F}$ is the graph of $\check{\chi}$. In summary, see the following diagram:

$$
\begin{array}{ccc}
(x, \xi) & \xrightarrow{\quad F:\chi \quad} & (y, \eta) \\
Q:C_Q \ \Big\updownarrow\ Q^{-1}:C_{Q^{-1}} & & \nearrow \\
& \check{F}=FQ^{-1}:\check{\chi} & \\
(\tilde{x}, \tilde{\xi}) & &
\end{array}
$$

For each given type of rank deficiency (here, in x_2) and each (x_0, ξ_0) within this class, there is an open set $O_{(x_0, \xi_0)}$ on which the coordinates (I, J) are valid (see Figure 2). These sets form an open cover, and we obtain a family of diffeomorphisms parametrized by (x_0, ξ_0); there exists a locally finite subcover, and we need only a discrete set to resolve the rank deficiencies everywhere. We index these by $j = 1, \ldots, N_i$ and construct a set of diffeomorphisms, $\{Q_{ij}\}_{j=1}^{N_i}$, which locally resolve the rank deficiency leading to coordinates (y, x_{I_i}, ξ_{J_i}). We write

$$
\begin{array}{ccc}
(y, x_{I_i}, \xi_{J_i}) & \xrightarrow{\ \kappa_{ij}\ } & (y, \tilde{\xi}) \\
\uparrow \downarrow r & & \uparrow \downarrow \tilde{r} \\
\Lambda \ni r = (y, \eta; x, \xi) & \xrightarrow{\ C_{Q_{ij}}\ } & (y, \eta; \tilde{x}, \tilde{\xi}) = \check{r} \in \check{\Lambda}_{ij}.
\end{array}
$$

We write $\check{O}_i$ for the image of O_i under the diffeomorphism on the level of Lagrangians. Let the matrix $\frac{\partial^2 \check{S}_{ij}}{\partial y \partial \tilde{\xi}}$ in the above be nonsingular on the open set $\check{U}_{ij}$, and introduce
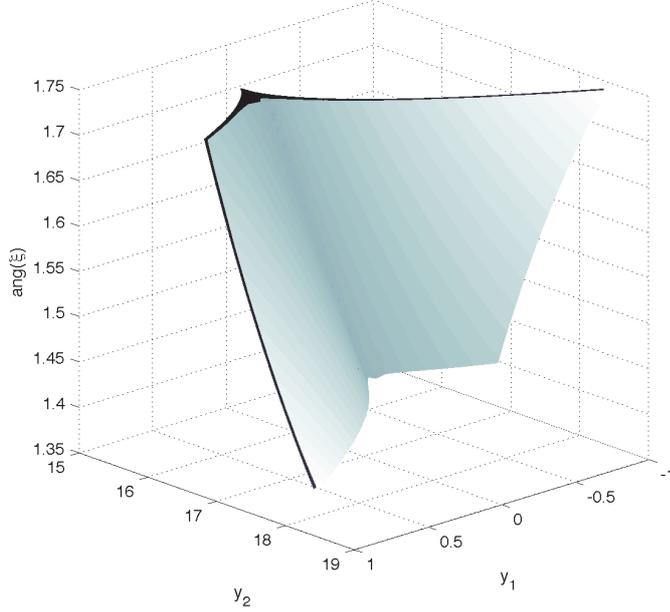
FIG. 2. *Caustic surfaces $\Xi(y, \xi)$ (dark gray) and $\check{\tilde{\Xi}}(y, \xi)$ (light gray) of Λ and $\check{\Lambda}$ corresponding to propagation through a low velocity lens (cf. section 5): The singular regions of Λ and $\check{\Lambda}$ do not intersect.*

$\check{O}_{ij} = \check{U}_{ij} \cap \check{O}_i \subset \check{\Lambda}_{ij}$. This set corresponds with a set $O_{ij} \subset \Lambda$. We subpartition $O_i = \cup_{j=1,\dots,N_i} O_{ij}$. The corresponding partition of unity now reads

$$(3.4) \quad \sum_{i=1}^{N} \sum_{j=1}^{N_i} \Gamma_{ij}(r) = 1, \quad \text{while } \bar{\Gamma}_{ij}(y, x_{I_i}, \xi_{J_i}) = \Gamma_{ij}(r(y, x_{I_i}, \xi_{J_i})), \ j = 1, \dots, N_i.$$

Then $(F\varphi_\gamma)(y) = \sum_{i=1}^{N} \sum_{j=1}^{N_i} (F_{ij}\varphi_\gamma)(y)$ with

(3.5)

$$(F_{ij}\varphi_\gamma)(y) = \iint \bar{\Gamma}_{ij}(y, x_{I_i}, \xi_{J_i}) a_i(y, x_{I_i}, \xi_{J_i}) \exp[i(S_i(y, x_{I_i}, \xi_{J_i}) - \langle \xi_{J_i}, x_{J_i} \rangle)] \, \varphi_\gamma(x) \mathrm{d}x \mathrm{d}\xi_{J_i}.$$

Inserting the diffeomorphisms, we obtain

$$(3.6) \qquad (F_{ij}\varphi_\gamma)(y) = \int \check{A}_{ij}(y, \tilde{\xi}) \exp[i\check{S}_{ij}(y, \tilde{\xi})] \, \widehat{Q_{ij}^* \varphi_\gamma}(\tilde{\xi}) \, \mathrm{d}\tilde{\xi}.$$

The amplitude $\check{A}_{ij}(y, \tilde{\xi})$ and phase function $\check{S}_{ij}(y, \tilde{\xi}) - \langle \tilde{\xi}, \tilde{x} \rangle$ are obtained by composing F_{ij} with Q_{ij}^{-1} as Fourier integral operators and changing phase variables. It is possible to treat this composition from a semigroup point of view. Then, to leading order, we get

$$(3.7) \qquad \check{A}_{ij}(y, \tilde{\xi}) = \bar{\check{\Gamma}}_{ij}(y, \tilde{\xi}) \, \check{a}_{ij}(y, \tilde{\xi}),$$

where

$$(3.8) \qquad \bar{\check{\Gamma}}_{ij}(y, \tilde{\xi}) = \check{\Gamma}_{ij}(\check{r}(y, \tilde{\xi})),$$

in which

$$(3.9) \qquad \check{\Gamma}_{ij}(\check{r}(r)) = \Gamma_{ij}(r).$$

Moreover, $\check{a}_{ij}(y, \tilde{\xi})$ can be obtained as follows. If Π is the propagator matrix of the perturbations of χ, then the propagator matrix of the perturbations of $\check{\chi}$ is given by $\check{\Pi}_{ij} = \Pi \, \Pi_{Q_{ij}}^{-1}$. Then

$$(3.10) \qquad \check{a}_{ij}(y, \tilde{\xi}) = \sqrt{1 / \det\left(\frac{\partial \check{S}_{ij}(y, \tilde{\xi})}{\partial y \partial \tilde{\xi}}\right)^{-1}},$$

where $\det\left(\frac{\partial \check{S}_{ij}(y, \tilde{\xi})}{\partial y \partial \tilde{\xi}}\right)^{-1}$ is obtained as the determinant of the upper-left subblock of $\check{\Pi}_{ij}$. To accommodate a common notation, we set $Q_{ij} = \mathbb{I}$ ($N_i = 1$) if $I_i = \emptyset$ and write Q_i. In the further analysis, we omit the subscripts $_i$ and $_{ij}$ where appropriate.

Expansion of the cutoff functions. To numerically evaluate (3.6) in reasonable time, we will use separated (in y and $\tilde{\xi}$) representations of $\check{A}_{ij}(y, \tilde{\xi})$ and $\check{S}_{ij}(y, \tilde{\xi})$ [2, 10, 11]. Such representations can be obtained by restricting the integration over $\tilde{\xi}$ to domains following a dyadic parabolic decomposition. Here, these will be given by the boxes $B_{\nu,k}(\tilde{\xi})$ following the redecomposition of $Q^* \varphi_\gamma$ into wave packets $\varphi_{\tilde{\gamma}}$, $Q^* \varphi_\gamma = \sum_{\tilde{\gamma}} u_{\tilde{\gamma}} \varphi_{\tilde{\gamma}}$. The key novelty is constructing a separated representation of the partition functions.

Consider our oscillatory integral in $(y, \tilde{\xi})$ including the cutoff $\bar{\check{\Gamma}}(y, \tilde{\xi})$. $\bar{\check{\Gamma}}(y, \tilde{\xi})$ is homogeneous of degree zero in $\tilde{\xi}$ and is a classical smooth symbol (of order 0). We "subdivide" the integration over $\tilde{\xi}$. A possible procedure involves obtaining a (low-rank) separated representation of $\bar{\check{\Gamma}}(y, \tilde{\xi})$ on the support of each relevant box in $\tilde{\xi}$ [3, 5, 4],

$$(3.11) \qquad \bar{\check{\Gamma}}(y, \tilde{\xi}) = \sum_{\beta=1}^{J_{\nu,k}} \check{\Gamma}_1^\beta(y) \check{\Gamma}_2^\beta(\tilde{\xi}), \quad \tilde{\xi} \in B_{\nu,k}.$$

(Basically, this can be obtained using spherical harmonics in view of the fact that the $\tilde{\xi}$ is implicitly limited to an annulus.) One can view this also as windowing the directions of $\tilde{\xi}$ into subsets (cones) using $\check{\Gamma}_2^\beta(\tilde{\xi})$ and then constructing $\check{\Gamma}_1^\beta(y)$ according to the smallest admissible set in y for the β-range of directions.

The oscillatory integral becomes

$$(3.12) \quad (F\varphi_\gamma)(y) = \sum_{\nu,k} \sum_{\beta=1}^{J_{\nu,k}} \check{\Gamma}_1^\beta(y) \int \check{a}(y, \tilde{\nu}) \exp[\mathrm{i}\check{S}(y, \tilde{\xi})] \, \check{\Gamma}_2^\beta(\tilde{\xi}) \, |\hat{\chi}_{\nu,k}(\tilde{\xi})|^2 \, \widehat{Q^* \varphi_\gamma}(\tilde{\xi}) \mathrm{d}\tilde{\xi}.$$

One can view $\check{\Gamma}_2^\beta(\tilde{\xi})\hat{\chi}_{\nu,k}(\tilde{\xi})$ as a subdivision of the box $B_{\nu,k}$. We know that $|J_{\nu,k}| \to 1$ as $k \to \infty$ since the cone of directions in $B_{\nu,k}$ shrinks as $\sqrt{k}$. Hence, for large k this does not involve any action.

The procedure allows a subdivision for coarse scales, as long as the scaling is not affected for large k. If the subdivision is too "coarse," then parts of the integration will be lost.

4. Computation. We describe an algorithm for applying Fourier integral operators in the above constructed universal oscillatory integral representation. The global hierarchy of operations is given by the following steps:

1. *Preparation step.* Preparation of universal oscillatory integral representation:
    (a) determination of open sets with local coordinates I_i, J_i on canonical relation Λ, inducing Q_{ij};
    (b) construction of cutoff functions $\check{\Gamma}_{ij}$ for the locally singularity-resolving diffeomorphisms Q_{ij};
    (c) construction of separated representation for $\check{\Gamma}_{ij}$.
2. *Evaluation of diffeomorphisms* $(Q_{ij}^* \varphi_\gamma)(\tilde{x})$.
3. *Evaluation of actions of* $(\check{F}_{ij}(Q_{ij}^* \varphi_\gamma))(y)$.

Step 3 requires the evaluation of the action of Fourier integral operators associated with canonical graphs in microlocal standard focal coordinates. The choice of discretization and algorithm for step 3 determines how computations in steps 1 and 2 are to be organized. Here, we perform computations in the almost symmetric wave packet transform domain. We make use of the "box-algorithm" computation of the action of Fourier integral operators associated with canonical graphs in microlocal standard focal coordinates $(y, \tilde{\xi})$ [2]. The box algorithm is based on the discretization and approximation, to accuracy $\mathcal{O}(2^{-k/2})$, of the action of $\check{F}_{ij}$ on a wave packet $\varphi_{j,\tilde{\nu},k}(\tilde{x})$,

$$(4.1) \qquad (\check{F}_{ij}\varphi_{\tilde{\gamma}})(y) \approx \check{A}(y,\tilde{\nu}) \sum_{r=1}^{R} \alpha_{\tilde{\nu},k}^{(r)}(y) \sum_{\tilde{\xi} \in B_{\tilde{\nu},k}} e^{i\langle T_{\tilde{\nu},k}(y), \xi\rangle} |\hat{\chi}_{\tilde{\nu},k}(\tilde{\xi})|^2 \hat{\vartheta}_{\tilde{\nu},k}^{(r)}(\tilde{\xi}).$$

The procedure relies on truncated Taylor series expansions of $\check{S}_{ij}(y,\tilde{\xi})$ and $\check{A}(y,\tilde{\xi})$ near the microlocal support of $\varphi_{\tilde{\gamma}}$, along the $\tilde{\nu} = \tilde{\xi}'/|\tilde{\xi}'|$ axis and in the $\tilde{\xi}''$ directions perpendicular to the radial $\tilde{\nu} = \tilde{\xi}'$ direction. Here, $T_{\tilde{\nu},k}(y)$ is the backwards solution

$$x(y) = T_{\tilde{\nu},k}(y) = \frac{\partial \check{S}_{ij}(y,\tilde{\nu})}{\partial \tilde{\xi}},$$

and $\alpha_{\tilde{\nu},k}^{(r)}(y)$ and $\vartheta_{\tilde{\nu},k}^{(r)}(\tilde{\xi})$ are functions realizing, on $B_{\tilde{\nu},k}$, a separated tensor-product representation of the slowly oscillating kernel appearing in the second-order expansion term of $\check{S}_{ij}$,

$$(4.2) \qquad \exp\left[i\frac{1}{2\tilde{\xi}'}\left\langle \tilde{\xi}'', \frac{\partial^2 \check{S}_{ij}}{\partial \tilde{\xi}''^2}(y,\tilde{\nu})\,\tilde{\xi}''\right\rangle\right] B_{\tilde{\nu},k}(\tilde{\xi}) \approx \sum_{r=1}^{R} \alpha_{\tilde{\nu},k}^{(r)}(y) \hat{\vartheta}_{\tilde{\nu},k}^{(r)}(\tilde{\xi}),$$

constructed from prolate spheroidal wave functions [6, 21, 22, 23, 27]. The number R of expansion terms is controlled by the prescribed accuracy ε of the tensor product representation. For a detailed description of the box-algorithm and its implementation, we refer the reader to [2].

Based on this tensor product representation, it is possible to group computations and to evaluate the action of $\check{F}_{ij}$ in step 3 for all data wave packets of the same frequency box $B_{\tilde{\nu},k}$ at once instead of for each φ_γ individually. Consequently, steps 1 and 2 will also be organized in terms of frequency boxes $B_{\tilde{\nu},k}$. We write $u_{\tilde{\nu},k}(\tilde{x}) = \sum_m u_{m,\tilde{\nu},k}\varphi_{m,\tilde{\nu},k}(\tilde{x})$ for the data portion corresponding to a frequency box $B_{\tilde{\nu},k}$. Starting from data $u(x)$, each of the following steps are repeated for any frequency box $B_{\nu,k}$ of interest.

4.1. Preparation step. We begin with determining the sets O_i for the box $B_{\nu,k}$. To this end, we compute the integral curves $(y(x,\xi), \eta(x,\xi))$ and their perturbations with respect to initial conditions (x,ξ) and monitor the null space of the matrix $\frac{\partial y}{\partial x}$ following section 2.2. For parametrices of evolution equations, this involves solving the system (2.6) and evaluating the propagator matrices $\Pi(x,\xi)$ by solving system (2.8). We evaluate the system of differential equations (2.8) in Fermi (or ray-centered) coordinates, in which the potential rank deficiencies of the upper left subblock $W_1(x,\xi)$ appear explicitly as zero entries in the corresponding row(s) and column(s) [25]. The submanifolds $\Sigma_{(x,\xi)}$ on which W_1 is singular separate and define the sets O_i. These computations on Λ_F are performed by discretizing the set of orientations $\nu = \xi/|\xi|$ covering the frequency box $B_{\nu,k}$ with resolution δ_ν and the set in x for which $u_{\nu,k}(x)$ has nonzero energy with resolution δ_x.

Then, for each set O_i, we detect $\check{U}_{ij}$ (and consequently $\check{O}_{ij}$) in a similar way, as the set on which the upper-left subblock $\check{W}_{1,ij}$ of $\check{\Pi}_{ij} = \Pi \, \Pi_{Q_{ij}}^{-1}$ has full rank. Here $\Pi_{Q_{ij}}^{-1}(\tilde{x}, \tilde{\xi})$ is given by (3.3). The operators Q_{ij} are chosen such that $\{\check{O}_{ij}\}_{j=1}^{N_i}$ overlappingly cover the set of singularities. For fixed α_i, this induces a discrete set $\{x_0^j\}_{j=1}^{N_i}$.

We then proceed with the construction of the partition of unity. Since the partition functions enter the computation as pseudodifferential cutoffs in the construction of the amplitude (cf. (3.7)), requiring the backwards solutions $\tilde{x}(y, \tilde{\xi})$ (compare (2.10)–(2.13)), we perform our numerical construction in coordinates $(\tilde{x}, \tilde{\xi})$. We obtain $\check{\Gamma}_{ij}(y, \tilde{\xi})$ upon substituting $y = y(\tilde{x}, \tilde{\xi})$ implied by the canonical relation $\check{\chi}_{ij}$. For the construction of the partition functions $\check{\Gamma}_{ij}$, we choose double-exponential cutoffs of the form

$$\exp(-\exp(d(\tilde{x}, \tilde{\xi}))),$$

mimicking a C_0^∞ cutoff, with appropriate normalization and truncated to precision ε. Here $d(\tilde{x}, \tilde{\xi})$ is a function measuring the distance of the point $(\tilde{x}, \tilde{\xi})$ from the boundary $\partial \check{U}_{ij}$ of the set $\check{U}_{ij}(\tilde{x}, \tilde{\xi})$. The partition of unity is then formed by weighting $\check{\Gamma}_{ij}(\tilde{x}, \tilde{\xi})$ on the overlaps of the sets $\check{U}_{ij}(\tilde{x}, \tilde{\xi})$ such that $\sum_{ij} \check{\Gamma}_{ij}(\check{r}(\tilde{x}, \tilde{\xi})) = 1$.

Finally, we construct the separated representations of $\check{\Gamma}_{ij}$ (cf. (3.12)) in $(\tilde{x}, \tilde{\xi})$ coordinates by windowing the directions of $\tilde{\xi}$ into subsets using $\check{\Gamma}_2^\beta(\tilde{\xi})$, realizing a subdivision into $\tilde{\xi}$ cones. This subdivision is performed for each frequency box $B_{\tilde{\nu},k}$.

4.2. Evaluation of diffeomorphisms. We evaluate each of the operators Q_{ij} in the Fourier domain. This choice is guided by the property $\sum_m u_{m,\nu,k} \hat{\varphi}_{m,\nu,k}(\xi) = \hat{u}(\xi) \hat{\beta}_{\nu,k}(\xi) \hat{\chi}_{\nu,k}(\xi)$ of the discrete almost symmetric wave packet transform [13], which enables the fast evaluation of the Fourier transform of the data at a set of frequency points $\xi_l^{\nu,k}$ limited to the box $B_{\nu,k}$. We obtain $(Q_{ij}^* \varphi_\gamma)(\tilde{x})$ at once for all $\varphi_\gamma(x)$ belonging to the frequency box $B_{\nu,k}$ by evaluation of their adjoint unequally spaced FFT [16, 17], $\mathcal{F}_{\xi \to x}^{US*}$, at points $x(\tilde{x}) = Q_{ij}^{-1}(\tilde{x})$,

$$\check{u}_{\nu,k}^{ij}(\tilde{x}) = \sum_m u_{m,\nu,k}(Q_{ij}^* \varphi_{m,\nu,k})(\tilde{x}) = \mathcal{F}_{\xi = \xi_l^{\nu,k} \to x(\tilde{x})}^{US*} \left[\hat{u}(\xi) \hat{\beta}_{\nu,k}(\xi) \hat{\chi}_{\nu,k}(\xi) \right].$$

In preparation for the evaluation of $(\check{F}_{ij} \check{u}_{\nu,k})(y)$, we compute the discrete almost symmetric wave packet transform of the pull back $\check{u}_{\nu,k}^{ij}(\tilde{x})$, yielding its wave packet coefficients $u_{\beth,\tilde{\nu},k}^{ij}$.

δ_ν, δ_x	Discretization steps in computations on Λ_F and $\check{\Lambda}_{ij}$
α_i	Free parameter of operators Q_{ij}, inducing the discrete sets of diffeomorphisms $\{Q_{ij}\}_{j=1}^{N_i}$
$J_{\nu,k}$	Number of expansion terms in separated representation of cutoff functions $\check{\Gamma}(y, \tilde{\xi})$
ϵ	Precision of approximate redecomposition of $\check{u}_{\nu,k}^{ij}(\tilde{x})$
ε	Accuracy of the tensor-product representation in the box algorithm

4.3. Evaluation of the actions of F_{ij}. At this stage, we are ready to evaluate the action $(F_{ij}u_{\nu,k})(y) = \sum_m u_{m,\nu,k}(F_{ij}\varphi_{m,\nu,k})(y)$ (cf. (3.6)) by evaluation of $(\check{F}_{ij}\check{u}_{\nu,k}^{ij})(y)$ using the box algorithm (cf. (4.1)). Note that numerically significant coefficients $u_{\mathbf{J},\tilde{\nu},k}^{ij}$ of the pull back $\check{u}_{\nu,k}^{ij}(\tilde{x})$ are contained in a small set of boxes $B_{\tilde{\nu},k}$ neighboring the direction $\nu = \xi_0/|\xi_0|$. We further subdivide each of these boxes according to the separated representation of $\check{\Gamma}_{ij}$. Then, we apply the box algorithm to each subdivision, indexed by triples $(\beta, \tilde{\nu}, k)$, $\beta = 1, \ldots, J_{\tilde{\nu},k}$. Here, the Taylor series expansion of the generating function $\check{S}_{ij}(y, \tilde{\xi})$ is constructed about the central $\tilde{\xi}$ direction within the support of $\Gamma_2^\beta(\tilde{\xi})\hat{\chi}_{\tilde{\nu},k}(\tilde{\xi})$, accounting for the induced subdivision of the box $B_{\tilde{\nu},k}$. Note that subdividing into $\tilde{\xi}$ cones results in a reduction of the range of $\tilde{\xi}$ orientations in each element $(\beta, \tilde{\nu}, k)$ of the subdivision, as compared to the $\tilde{\xi}$ range contained in $B_{\tilde{\nu},k}$. This reduces the number R of expansion terms in (4.1) and effectively counter-balances the increase by a factor $J_{\tilde{\nu},k}$, evoked by the separated representation of $\check{\Gamma}_{ij}$, of the number of times the box-algorithm has to be applied.

Operator hierarchy. The operators F_{ij} for which $Q_{ij} = \mathbb{I}$, $F_{ij}^{(\mathbb{I})}$ say, are directly associated with the canonical relation Λ_F and involve only computations on Λ_F. In the algorithm, we reflect this physical hierarchy of the operators F_{ij} in the construction of the partition of unity. First, we construct a partition of unity for these hierarchically higher operators. Then, we construct a joint partition of the remaining operators on the sets which are not covered by the sets for which $Q_{ij} = \mathbb{I}$.

Redecomposition. Starting from a single box $B_{\nu,k}$ and applying Q_{ij} to $u_{\nu,k}(x)$, redecomposition of $\check{u}_{\nu,k}^{ij}(\tilde{x})$ results in a set of boxes $B_{\tilde{\nu},k}$ yielding numerically nonzero contribution to the solution. The number of boxes entering the computation is directly proportional to the computational cost of the algorithm. In applications, we therefore aim at keeping this number small and consider only a subset of boxes, yielding the most significant contributions. We choose this subset such that on an open neighborhood of (x_0, ξ_0),

$$Q_{ij}^{-1}Q_{ij} \approx \mathbb{I}$$

to precision ϵ. We can estimate the energy loss induced by the restriction to subsets of $B_{\tilde{\nu},k}$ and renormalize the solution. We illustrate the impact of choices of subsets containing different numbers of boxes on the numerical accuracy of the diffeomorphic identity in Figure 3.

Furthermore, the redecomposition of $\check{u}_{\nu,k}^{ij}(\tilde{x})$ yields in general, under the action of Q_{ij}^{-1}, ξ-values outside the set $B_{\nu,k}$, $\xi(x, \tilde{\xi}) \supset B_{\nu,k}$. We monitor $\xi(x, \tilde{\xi})$ and do not consider their contribution in our computation if $|\hat{\chi}_{\nu,k}(\xi(x, \tilde{\xi}))|$ is below the threshold ε.

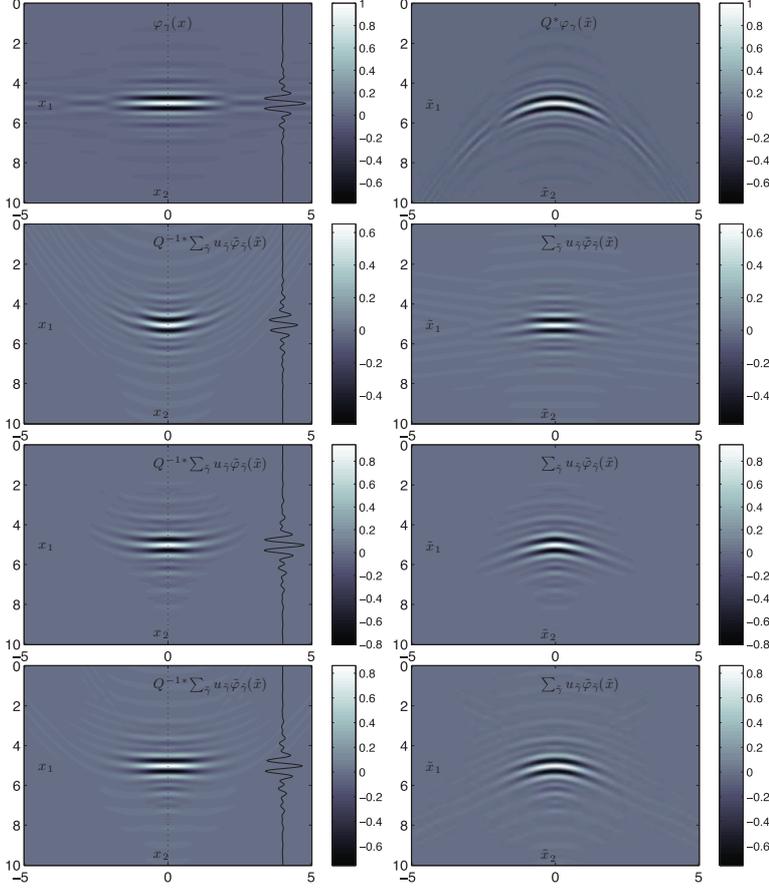The free parameters of the procedure are summarized in Table 4.1.

Fig. 3. *Illustration of diffeomorphism Q, Q^{-1} and redecomposition for a wave packet $\varphi_\gamma(x)$ at frequency scale $k = 2$. Top row: $\varphi_\gamma(x)$ (left) and pull back $Q^*\varphi_\gamma(\tilde{x})$ (right). Rows 2 to 4: Redecompositions $\sum_{\tilde{\nu},k} u_{\tilde{\gamma}}\tilde{\varphi}_{\tilde{\gamma}}(\tilde{x})$ of $Q^*\varphi_\gamma(\tilde{x})$ using 3, 7, and 9 boxes $B_{\tilde{\nu},k}$, respectively (right column), and the corresponding image $Q^{*-1}\big(\sum_{\tilde{\nu},k} u_{\tilde{\gamma}}\tilde{\varphi}_{\tilde{\gamma}}\big)(x)$ under the action of Q^{-1} (left column). An insufficient number of boxes alters the amplitudes and the minimum phase property of wave packets. Increasing the number of boxes yields satisfactory results in an open neighborhood of (x_0, ξ_0).*

5. Numerical example. We numerically illustrate our algorithm for the evaluation of the action of Fourier integral operators associated with evolution equations. We consider wave evolution under the half-wave equation, that is, the initial value problem (2.5) with symbol

$$P(x,\xi) = \sqrt{c(x)^2 \|\xi\|^2},$$

in $n = 2$ dimensions. Here $c(x)$ stands for the medium velocity.

Heterogeneous, isotropic model. We choose a heterogeneous velocity model,

$$c(x) = c_0 + \kappa \exp(-|x - x_0|^2/\sigma^2),$$

containing a low velocity lens, with parameters $c_0 = 2\,\text{km/s}$, $\kappa = -0.4\,\text{km/s}$, $\sigma = 3\,\text{km}$, and $x_0 = (0, 14)\,\text{km}$. As the initial data, we choose horizontal wave packets
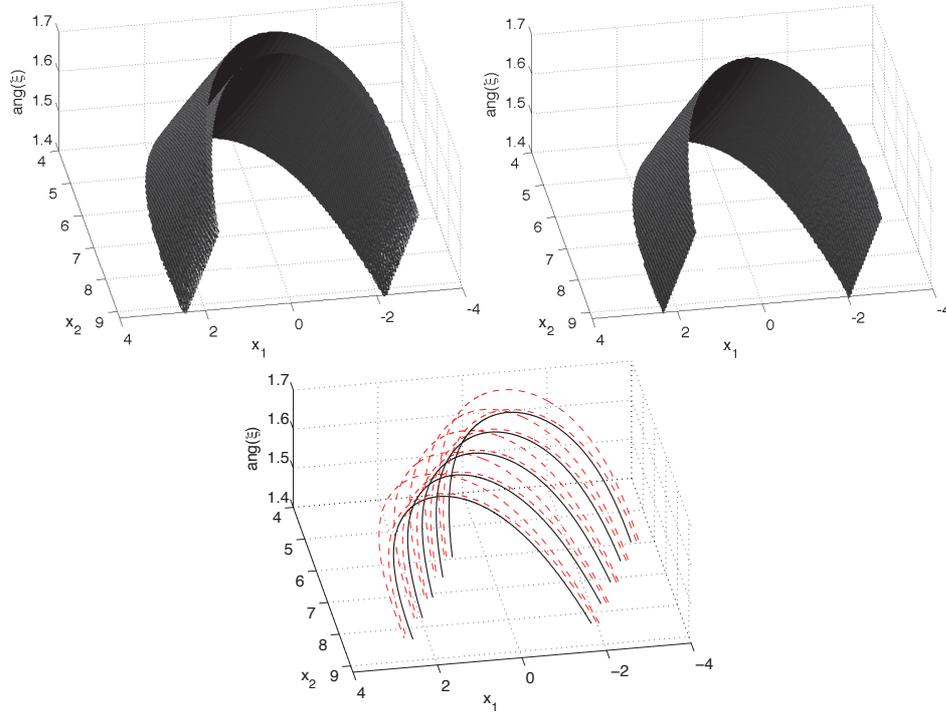
FIG. 4. *Top left: Iso-amplitude surface of the partition functions $\bar{\Gamma}_i(x,\xi)$, $i = 1,3$, associated with $Q_i = \mathbb{I}$: the joint admissible set $O_1 \cup O_3$ comprises the exterior of the two sheets. Top right: Iso-amplitude surface of $\bar{\Gamma}_{ij}(x(\tilde{x}, \tilde{\xi}), \xi(\tilde{x}, \tilde{\xi}))$ for $\xi_0 = \pi/2$, $x_{2,0} = 0$, and $\alpha = 1$ ($i = 2, j = 1$): the admissible set O_{ij} contains the region on the back of the sheet. Bottom: Boundaries ∂O_i, $i = 1,3$ (dashed curves), and ∂O_{ij}, $i = 2, j = 1$ (solid curves), of the admissible domains: clearly, the joint admissible set $O_1 \cup O_3 \cup O_{21}$ covers Λ.*
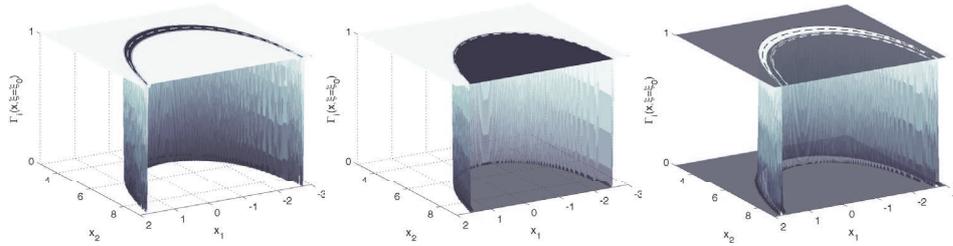

FIG. 5. *Illustration of joint partition of unity for the partition functions and sets in Figure 4 for $\xi_0 = 1.67$ fixed: Slice of $\bar{\Gamma}_i(x, \xi = \xi_0)$ (left), the admissible set U_{ij} and the associated partition function $\bar{\Gamma}_{ij}(x(\tilde{x}, \tilde{\xi}), \xi(\tilde{x}, \tilde{\xi}) = \xi_0)$ (center), and the partition function $\bar{\Gamma}_{ij}(x(\tilde{x}, \tilde{\xi}), \xi(\tilde{x}, \tilde{\xi}) = 1.67)$ for O_{ij} realizing the partition of unity with $\bar{\Gamma}_i(x, \xi = \xi_0)$.*

at frequency scale $k = 2$ and $k = 3$, respectively, in the vicinity of the point $x' = (0,5)$ km. We set $t_0 = 0$ and fix the evolution time to $T = 7$ s. With this choice of parameters, most of the energy of the solution is concentrated near a cusp-type caustic. We illustrate the induced sets O_i and the joint partition of unity Γ_i in Figures 4 and 5.
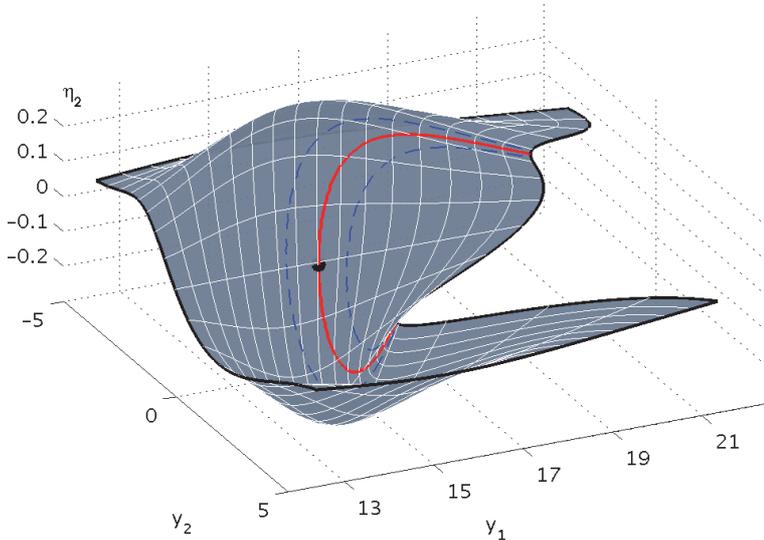
FIG. 6. *Projection $\bar{\Lambda}(y, \eta_2)$ of a slice $\xi = \xi_0$ of the canonical relation Λ associated with a half-wave equation in the vicinity of a caustic (red solid line; the blue dashed lines indicate the neighborhood of the singularity) caused by a low velocity lens. The white solid lines are connected to a regular grid in x by bicharacteristics. The black dot indicates the center of an open neighborhood of conjugate points $(x_0, \xi_0) \mapsto (y_0, \eta_0)$ for which the projection onto standard microlocal focal coordinates (y, ξ) is not diffeomorphic.*

Operator factorization. We partition the Lagrangian Λ into three sets O_i, $i = \{1, 2, 3\}$. The sets $i = \{1, 3\}$ are separated by the caustic. For these sets, we can choose coordinates (y, ξ); hence $Q_i = \mathbb{I}$. The set $i = 2$ contains the caustic. For illustration purposes, in the factorization F_{ij} of F_i for $i = 2$, we choose to compute the operator $j = 1$, which resolves the singularity in an open neighborhood of the point indicated by a black dot on the Lagrangian plotted in Figure 6. This neighborhood contains the cusp of the caustic. Furthermore, we limit our separated representation to one term, $J_{\nu,k} = 1$. (For the corresponding admissible sets and partition functions, see Figure 7(left column).) We restrict the computation of F_{ij} for the initial data at frequency scale $k = 2$ ($k = 3$) to 9 (11) boxes $B_{\tilde{\nu},k}$ neighboring the ν direction.

Results. In Figure 8, we plot the contributions of the different components in the factorization of the propagator acting on a single horizontal wave packet at frequency scale $k = 2$, and compare the results to a time domain finite difference computation. The support of the wave packet within the joint admissible set of the chosen factorization is mostly covered by the set O_{ij}, such that most of its energy is contributed by the operator F_{ij} for which $Q_{ij} \neq \mathbb{I}$.

We observe that, in the joint admissible set, our algorithm has effectively removed the singularity. We note that the phase of the operator computation matches the phase of the finite difference reference. This includes the KMAH index, which is best observed for operator F_3, which exclusively contributes to the region beyond the caustic (cf. Figure 8(top left)). Furthermore, note that the amplitude obtained by our algorithm is slightly weaker than the true amplitude. This is consistent with the observations and discussion following Figure 3 and results from the energy leakage induced by restricting the number of boxes in the redecomposition step following the
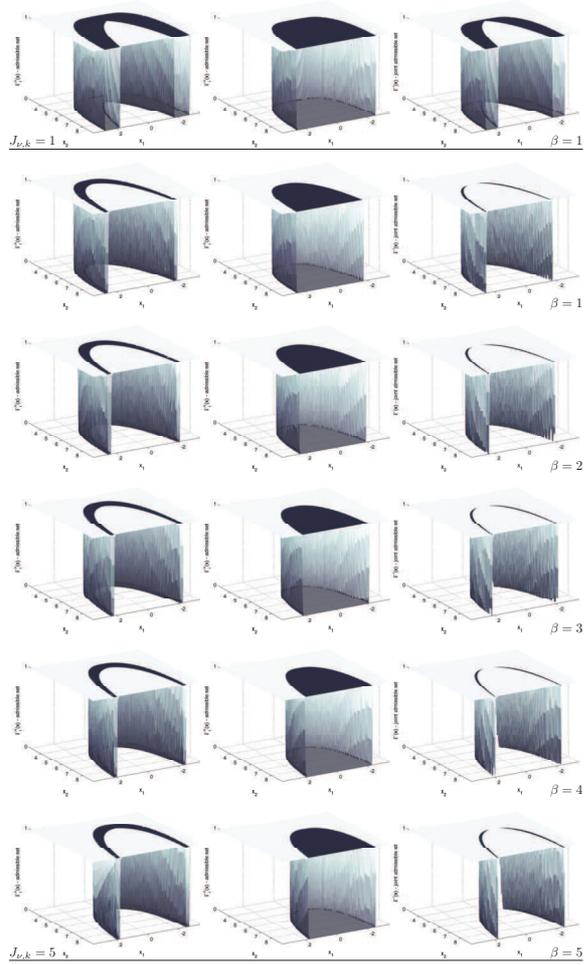
FIG. 7. *Illustration of admissible sets and expansion functions $\check{\Gamma}_1^\beta(y(x))$ in (3.11) with $J_{\nu,k} = 1$ (top row) and $J_{\nu,k} = 5$ (lower rows) for the partition functions in Figure 4. Left column: The partition functions $\bar{\Gamma}_i(y(x), \xi)$, $i = 1, 3$. Center column: The partition functions $\bar{\Gamma}_{ij}(y(\tilde{x}, \tilde{\xi}), \xi(\tilde{x}, \tilde{\xi}))$, $i = 2, j = 1$. Right column: The joint admissible sets induced by the partition of unity for the expansion functions plotted in the left and center columns.*

application of Q. We can compensate and renormalize the amplitude by monitoring the energy loss resulting from the restriction. (In Figure 8, we have not renormalized the amplitudes.) Finally, we note that our algorithm yields the correct result in an open neighborhood in the vicinity of the tip of the caustic, for which we have designed the operator F_{ij}. Consistent with this fact, the operator F_{ij} is ineffective for yielding the image of the entire wave packet which, at this low frequency scale, has support extending beyond the admissible set of the operator factors we compute.

These observations are further illustrated in Figure 9(left column), where we plot the contributions of the different components in the factorization of the propagator acting on horizontal wave packets, at higher frequency scale $k = 3$, centered at four different locations in the vicinity of the caustic tip. Results of a time domain finite
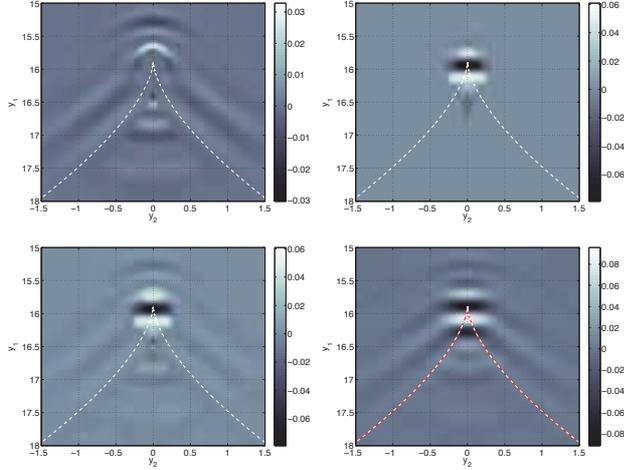
FIG. 8. *Illustration of operator action on a wave packet $\varphi_\gamma(x)$ at frequency scale $k = 2$: Contribution of operators F_i ($i = 1, 3$) associated with $Q_i = \mathbb{I}$ (top left), contribution of operator F_{ij} ($i = 2, j = 1$) with diffeomorphism parameters ($\xi_0 = \pi/2, x_{2,0} = 0, \alpha = 1$), resolving the singularity in the tip of the caustic (top right), and joint action of F_i and F_{ij} (bottom left). Time domain finite difference reference (bottom right). In the operator computation, we consider 9 boxes $B_{\tilde{\nu},k}$ and a separated representation with $J_{\nu,k} = 1$ term.*

difference reference computation are plotted in Figure 9(center column). With these initial data, we explore the open neighborhood about the point for which the operator composition with Q_{ij} resolves the singularity. Indeed, at this frequency scale, we can obtain the image of an entire wave packet with only one operator factor F_{ij} (cf. Figure 9(second row)). For the wave packet located slightly further above the tip of the caustic (top row), we observe a phase artifact in the region of overlap of $O_{i=1}$ and O_{ij}, which can be explained as follows: The restriction of the separated representation for F_i to only one term implies that the computation of the geometry (bicharacteristics) for the entire box $B_{\nu,k}$ is exclusively based on one single direction ν. This results in inaccuracies in regions close to the caustics where slight perturbations in ξ yield large variations in y. Furthermore, as discussed above, wave packets exploring the regions beyond the tip of the caustics eventually start to leave the admissible set for F_{ij} (third and bottom line).

We note that, both for removing the phase artifact of F_i close to the caustic and for enlarging the admissible set, it is necessary to increase the number of terms $J_{\nu,k}$ in the separated representation (3.11) (compare with Figure 7). This is illustrated in Figure 9(right column), where the joint contributions of operators F_i and F_{ij} with $J_{\nu,k} = 11$ terms in the separated representation are plotted. Here, the expansion functions $\check{\Gamma}_2^\beta(\tilde{\xi})$ are constructed as cones in $\tilde{\xi}$ with a squared cosine cutoff window. For practical reasons and illustration purposes, only one single frequency box $B_{\tilde{\nu},k}$ has been used in the computation (cf. Figure 3). While this restriction to only one frequency box affects the amplitudes and the phases in the tails of the wave packet, the separated representation remains nonetheless effective in resolving the issues observed above: the admissible set is extended beyond the caustic, and the inaccuracies in the regions of overlap of sets O_i and O_{ij} as well as in the regions close to the caustics are considerably reduced.
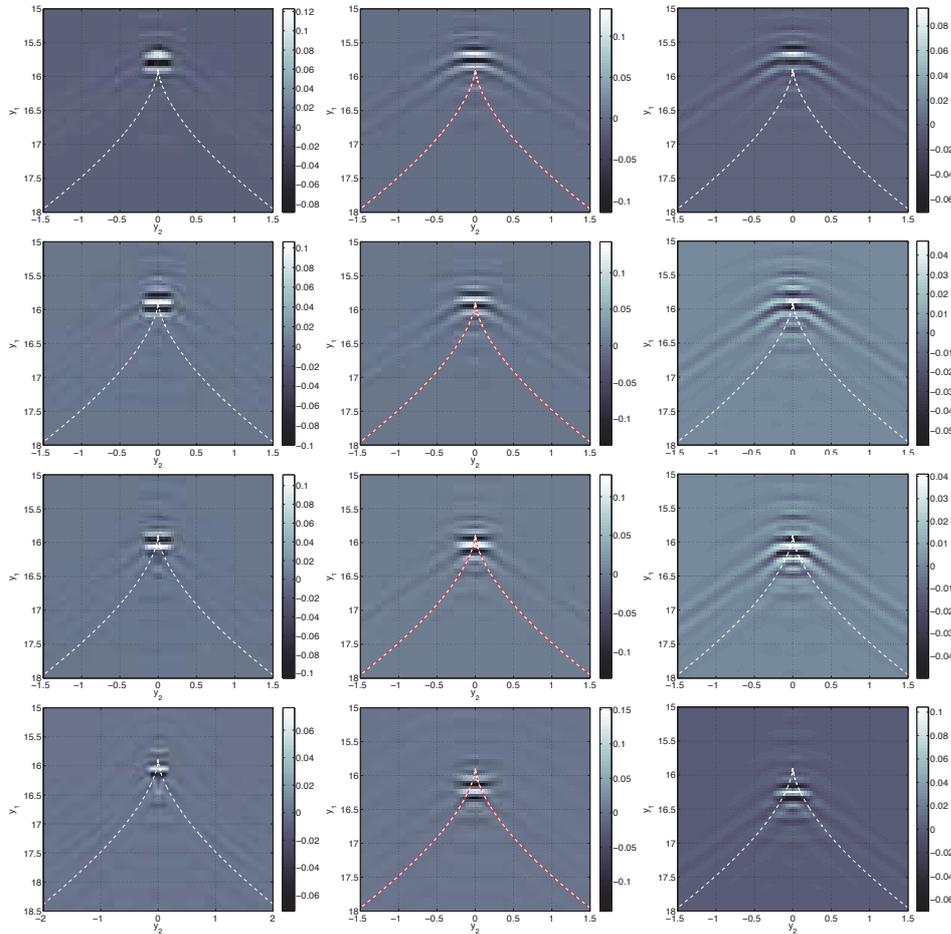
FIG. 9. *Left column: Joint contribution of the operators F_i and F_{ij} acting on a wave packet $\varphi_\gamma(x)$ at frequency scale $k = 3$ (compare with Figure 8(bottom left) for a wave packet at frequency scale $k = 2$). Center column: Time domain finite difference reference. Right column: The equivalent to the left column when using a separated representation with $J_{\nu,k} = 11$ terms. (Note that for computational reasons, only one box $B_{\tilde{\nu},k}$ has been used in the numerical evaluation of F_i and F_{ij} with $J_{\nu,k} = 11$ terms.)*

6. Discussion. We developed an algorithm for the evaluation of the action of Fourier integral operators through their factorization into operators with a universal oscillatory integral representation, enabled by the construction of appropriately chosen diffeomorphisms. The algorithm comprises a preparatory geometrical step in which open sets are detected on the canonical relation for which specific focal coordinates are admissible. This covering with open sets induces a pseudodifferential partition of unity. Then, for each term of this partition, we apply a factorization of the associated operators using diffeomorphisms reflecting the rank deficiency and resolving the singularity in the set. This factorization admits a parametrization of the canonical graph in universal $(y, \tilde{\xi})$ coordinate pairs and enables the application of our previously developed box algorithm, following the dyadic parabolic decomposition of phase space, for numerical computations. Hence, our algorithm enables the

discrete wave packet–based computation of the action of Fourier integral operators globally, including in the vicinity of caustics. This wave packet description is valid on the entire canonical relation. It can now be used with procedures aiming at the iterative refinement of approximate solutions, and it can drive the construction of weak solutions via Volterra kernels [1, 12].

An alternative approach for obtaining solutions in the vicinity of caustics has been proposed previously [2, 19, 20] for the special case of Fourier integral operators corresponding to parametrices of evolution equations for isotropic media. It consists of a redecomposition strategy following a multiproduct representation of the propagator. Here, we avoid the redecompositions and operator compositions following the discretization of the evolution parameter, reminiscent of a stepping procedure. What is more, our construction is not restricted to parametrices of evolution equations, but is valid for the general class of Fourier integral operators associated with canonical graphs, allowing for anisotropy. The cost of the algorithm resides in the construction and application of the separated representation of the pseudodifferential partition of unity.

REFERENCES

[1] F. ANDERSSON, M. V. DE HOOP, H. F. SMITH, AND G. UHLMANN, *A multi-scale approach to hyperbolic evolution equations with limited smoothness*, Comm. Partial Differential Equations, 33 (2008), pp. 988–1017.

[2] F. ANDERSSON, M. V. DE HOOP, AND H. WENDT, *Multiscale discrete approximation of Fourier integral operators*, Multiscale Model. Simul., 10 (2012), pp. 111–145.

[3] G. BAO AND W. W. SYMES, *Computation of pseudo-differential operators*, SIAM J. Sci. Comput., 17 (1996), pp. 416–429.

[4] G. BEYLKIN, V. CHERUVU, AND F. PÉREZ, *Fast adaptive algorithms in the non-standard form for multidimensional problems*, Appl. Comput. Harmon. Anal., 24 (2008), pp. 354–377.

[5] G. BEYLKIN AND M. J. MOHLENKAMP, *Algorithms for numerical analysis in high dimensions*, SIAM J. Sci. Comput., 26 (2005), pp. 2133–2159.

[6] G. BEYLKIN AND K. SANDBERG, *Wave propagation using bases for band-limited functions*, Wave Motion, 41 (2005), pp. 263–291.

[7] B. BRADIE, R. COIFMAN, AND A. GROSSMANN, *Fast numerical computations of oscillatory integrals related to acoustic scattering*, I, Appl. Comput. Harmon. Anal., 1 (1993), pp. 94–99.

[8] E. CANDÈS AND L. DEMANET, *Curvelets and Fourier integral operators*, C. R. Acad. Sci. Paris, 336 (2003), pp. 395–398.

[9] E. CANDÈS, L. DEMANET, D. DONOHO, AND L. YING, *Fast discrete curvelet transforms*, Multiscale Model. Simul., 5 (2006), pp. 861–899.

[10] E. CANDÈS, L. DEMANET, AND L. YING, *Fast computation of Fourier integral operators*, SIAM J. Sci. Comput., 29 (2007), pp. 2464–2493.

[11] E. CANDÈS, L. DEMANET, AND L. YING, *A fast butterfly algorithm for the computation of Fourier integral operators*, Multiscale Model. Simul., 7 (2009), pp. 1727–1750.

[12] M. V. DE HOOP, S. F. HOLMAN, H. F. SMITH, AND G. UHLMANN, *Regularity and multi-scale discretization of the solution construction of hyperbolic evolution equations with limited smoothness*, Appl. Comput. Harmon. Anal., 33 (2012), pp. 330–353.

[13] A. DUCHKOV, F. ANDERSSON, AND M. V. DE HOOP, *Discrete almost symmetric wave packets and multi-scale representation of (seismic) waves*, IEEE Trans. Geosci. Remote Sens., 48 (2010), pp. 3408–3423.

[14] A. DUCHKOV AND M. V. DE HOOP, *Extended isochron rays in shot-geophone (map) migration*, Geophys., 75 (2010), pp. 139–150.

[15] A. DUCHKOV, M. V. DE HOOP, AND A. SÁ BARETTO, *Evolution-equation approach to seismic image, and data, continuation*, Wave Motion, 45 (2008), pp. 952–969.

[16] A. DUTT AND V. ROKHLIN, *Fast Fourier transforms for nonequispaced data*, SIAM J. Sci. Comput., 14 (1993), pp. 1368–1393.

[17] A. DUTT AND V. ROKHLIN, *Fast Fourier transforms for nonequispaced data* II, Appl. Comput. Harmon. Anal., 2 (1995), pp. 85–100.

[18] L. HÖRMANDER, *The Analysis of Linear Partial Differential Operators, Vol.* IV, Springer-Verlag, Berlin, 1985.

[19] H. KUMANO-GO, K. TANIGUCHI, AND Y. TOZAKI, *Multi-products of phase functions for Fourier integral operators with an applications*, Comm. Partial Differential Equations, 3 (1978), pp. 349–380.

[20] J. H. LE ROUSSEAU, *Fourier-integral-operator approximation of solutions to first-order hyperbolic pseudodifferential equations* I: *Convergence in Sobolev spaces*, Comm. Partial Differential Equations, 31 (2006), pp. 867–906.

[21] D. SLEPIAN, *Prolate spheroidal wave functions, Fourier analysis and uncertainty—IV: Extensions to many dimensions, generalized prolate spheroidal wave functions*, Bell Syst. Tech. J., November (1964), pp. 3009–3057.

[22] D. SLEPIAN, *On the symmetrized Kronecker power of a matrix and extensions of Mehler's formula for Hermite polynomials*, SIAM J. Math. Anal., 3 (1972), pp. 606–616.

[23] D. SLEPIAN, *Prolate spheroidal wave functions, Fourier analysis and uncertainty—V: The discrete case*, Bell Syst. Tech. J., 57 (1978), pp. 1371–1430.

[24] H. SMITH, *A parametrix construction for wave equations with $C^{1,1}$ coefficients*, Ann. Inst. Fourier (Grenoble), 48 (1998), pp. 797–835.

[25] V. ČERVENÝ, *Seismic Ray Theory*, Cambridge University Press, Cambridge, UK, 2001.

[26] V. ČERVENÝ, *A note on dynamic ray tracing in ray-centered coordinates in anisotropic inhomogeneous media*, Stud. Geophys. Geod., 51 (2007), pp. 411–422.

[27] H. XIAO, V. ROKHLIN, AND N. YARVIN, *Prolate spheroidal wave functions, quadrature and interpolation*, Inverse Problems, 17 (2001), pp. 805–838.